Electronic Supplementary Material (ESI) for Nanoscale.

Supplementary information

Hollow mesoporous carbon nanospheres for imaging-guided light-activated synergistic thermo-chemotherapy

Yuwei Qiu[a], Dandan Ding[a], Wenjing Sun[a], Yushuo Feng[a], Doudou Huang[a], Sicheng Li[a], Shanshan Meng[a], Qingliang Zhao[a,*], Li-Jun Xue[b,*], Hongmin Chen[a,*]

[a]State Key Laboratory of Molecular Vaccinology and Molecular Diagnostics & Center for Molecular Imaging and Translational Medicine, School of Public Health, Xiamen University, Xiamen 361102, China

[b]Department of Medical Oncology, Jinling Hospital, Nanjing University Clinical School of Medicine, Nanjing, 210002, China

*Corresponding author:

zhaoql@xmu.edu.cn (Q.Z.); xue_lj@163.com (L.X.); hchen@xmu.edu.cn (H.C.)

Calculation of the photothermal conversion efficiency

The photothermal conversion efficiency of the HMCNs was determined by the Equation 1[1, 2]:

$$\eta = \frac{hS(T_{max} - T_{surr}) - Q_{Dis}}{I(1 - 10^{-A_\lambda})} \quad (1)$$

Where h is the heat-transfer coefficient, S is the surface area of the container, T_{max} is the equilibrium temperature, T_{surr} is room temperature, Q_{Dis} is the heat dissipation due to the light absorbed by the quartz sample cell, I is the laser power, and A_λ is the absorbance at an excitation wavelength of 808 nm. The value of hS was derived according to the following Equation 2:

$$hS = \frac{m_D C_D}{\tau_s} \quad (2)$$

Where τ_s is the sample system time constant, which can be obtained from Figure S3b, m_D and C_D are the mass (0.22 g) and heat capacity (4.2 J·g $^{-1}$) of deionized water, respectively. In order to gain hS, a dimensionless parameter is introduced:

$$\theta = \frac{T - T_{surr}}{T_{max} - T_{surr}} \quad (3)$$

And the sample system time constant $\tau_s$can be calculated as Equation 4:

$$t = -\tau_s ln(\theta) \quad (4)$$

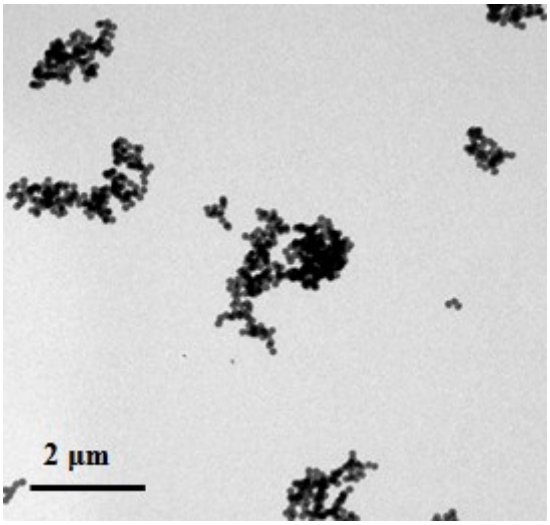

Fig. S1 The TEM image of BCPs.

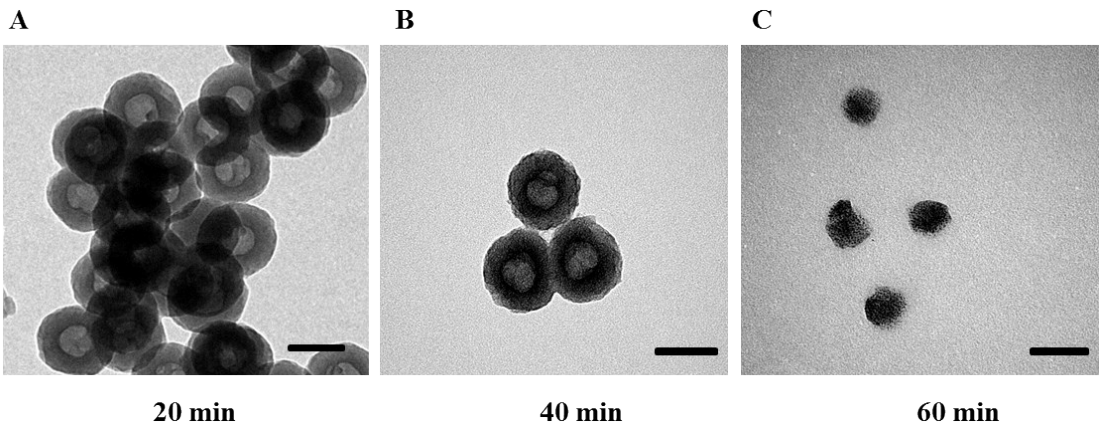

Fig. S2 The TEM images of BCPs after HNO_3 treatment with (A) 20 min, (B) 40 min and (C) 60 min, respectively (Scale bar: 100 nm).

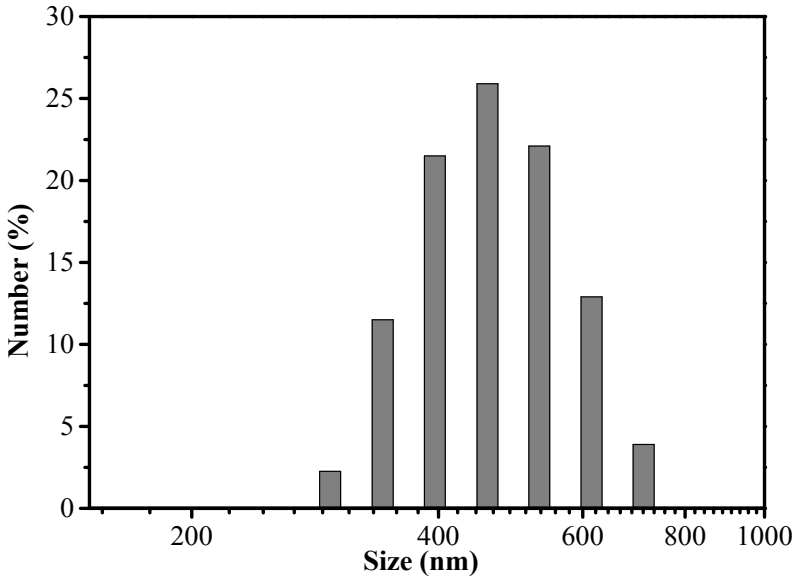

Fig. S3 Size distribution of BCPs in water.

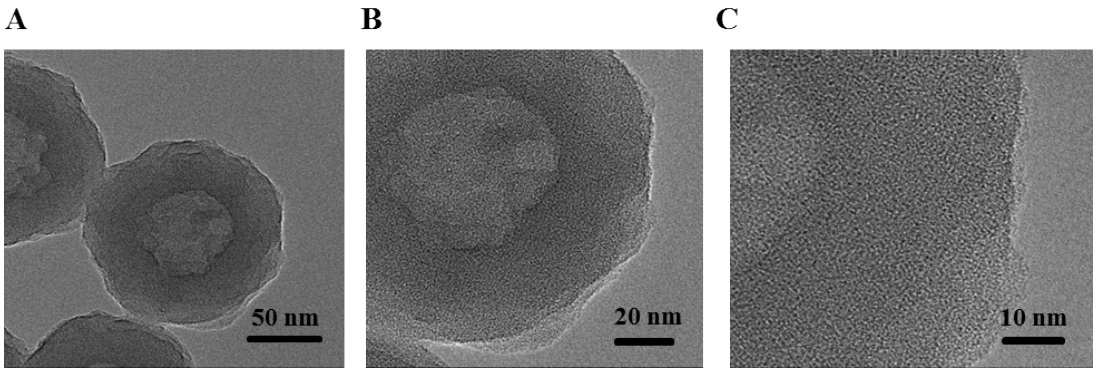

Fig. S4 HR-TEM images of HMCNs.

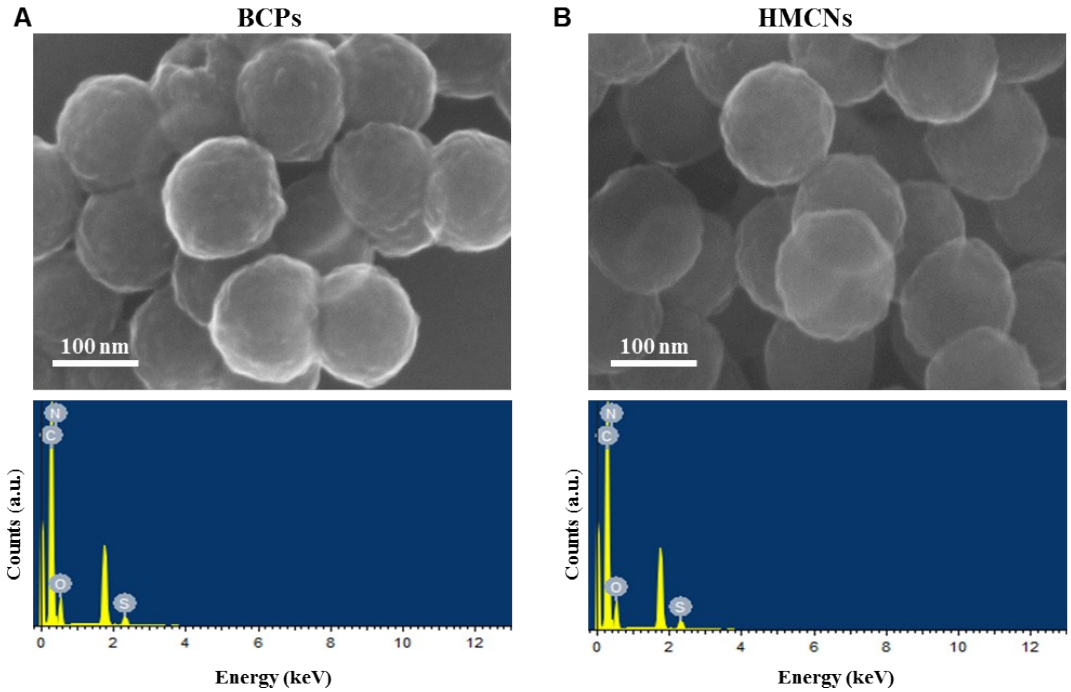

Element	Weight %	Atomic %
C(K)	61.85	67.15
N(K)	17.40	16.20
O(K)	20.09	16.38
S(K)	0.67	0.27

Element	Weight %	Atomic %
C(K)	49.66	55.30
N(K)	23.16	22.12
O(K)	26.84	22.44
S(K)	0.34	0.14

Fig. S5 SEM images and EDX spectra of (A) BCPs and (B) HMCNs.

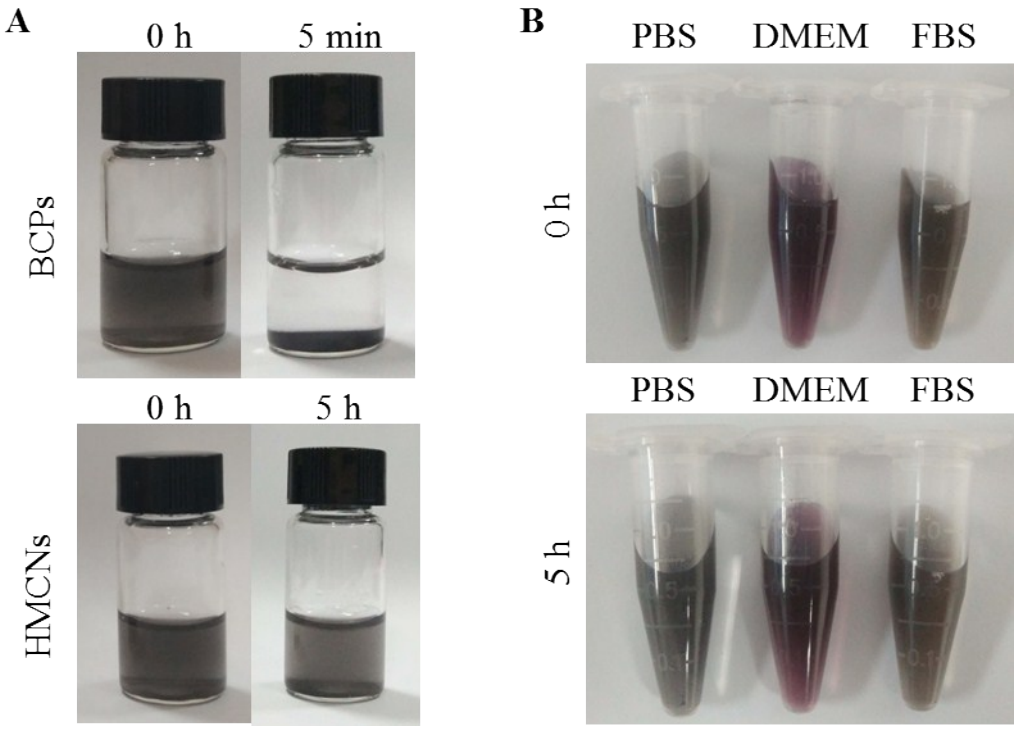

Fig. S6 (A) Photograph of BCPs and HMCNs dispersed in water at different time points. (B) The stability of HMCNs (100 μg/mL) in different medium in 5 h.

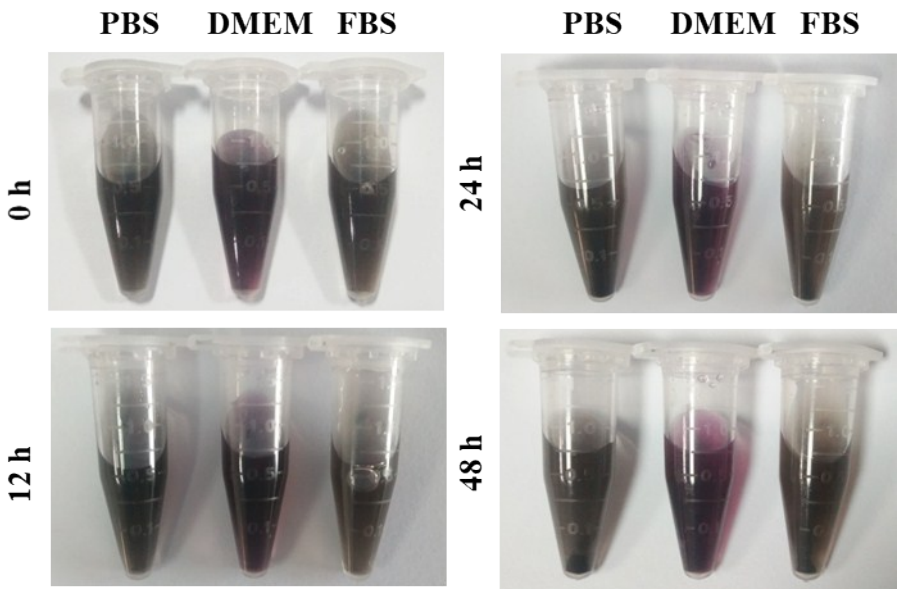

Fig. S7 The stability of HMCNs (100 μg/mL) in different medium with 12, 24, 48 h.

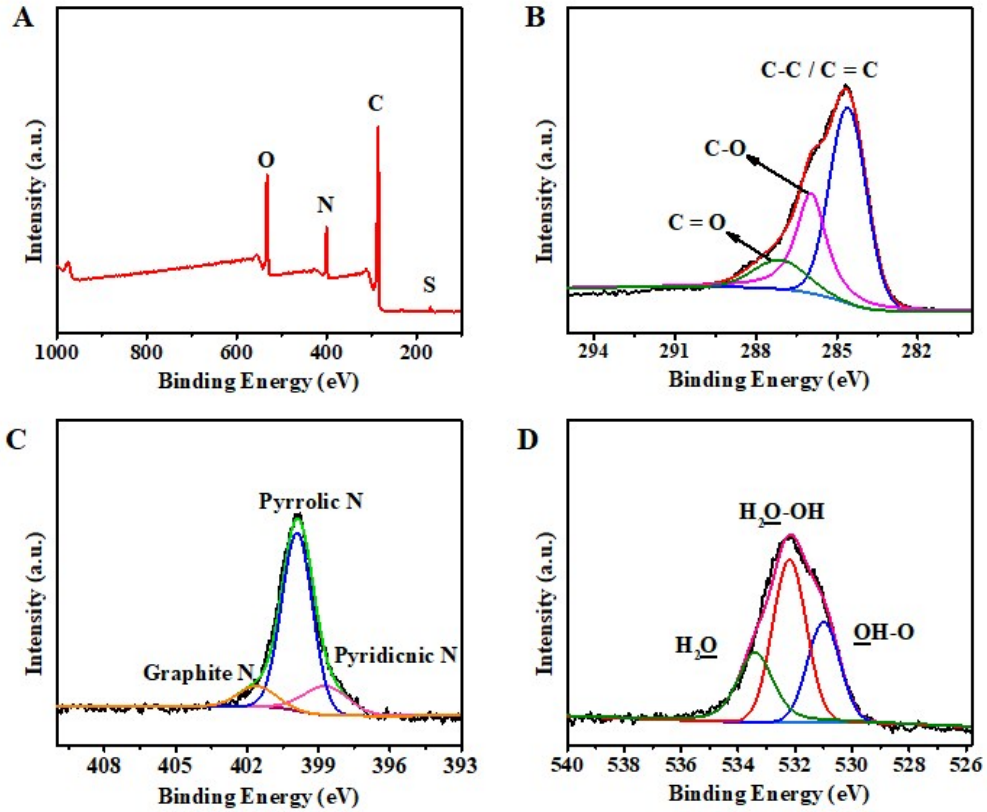

Fig. S8 (A) The full-scan XPS spectrum of HMCNs. (B) High-resolution C1s scan. (C) High-resolution N1s scan. (D) High-resolution O1s scan.

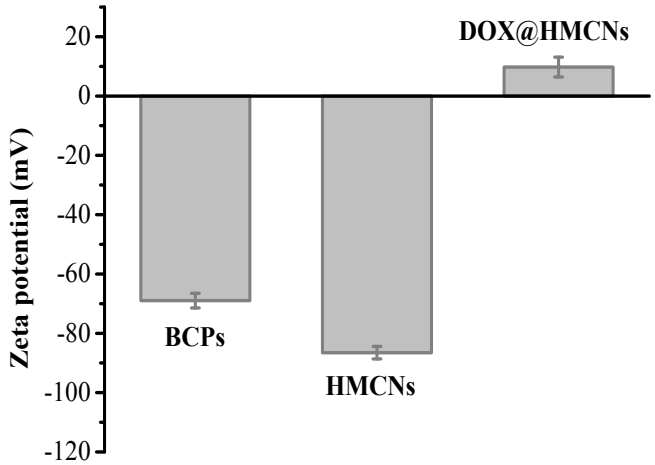

Fig. S9 Zeta potential of original BCPs, HMCNs, and DOX@HMCNs.

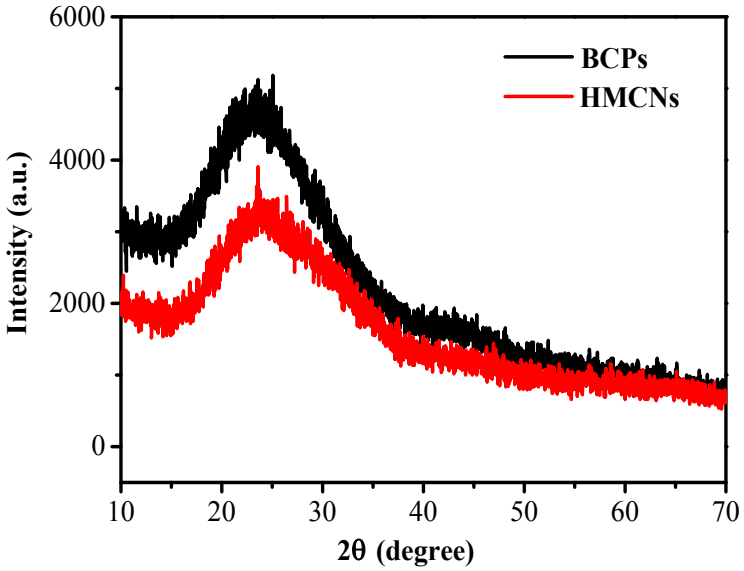

Fig. S10 XRD patterns of BCPs, HMCNs.

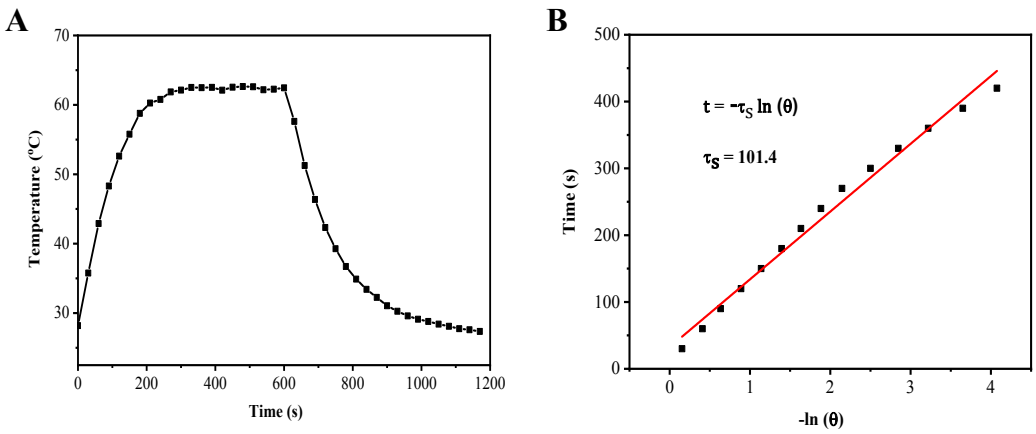

Fig. S11 (A) Photothermal response of HMCNs aqueous dispersion (100 μg·mL^{-1}, 200 μL) under 808 nm laser irradiation. (B) Calculation of the time constant for heat transfer using a linear regression obtained from the cooling period of Fig. S11A.

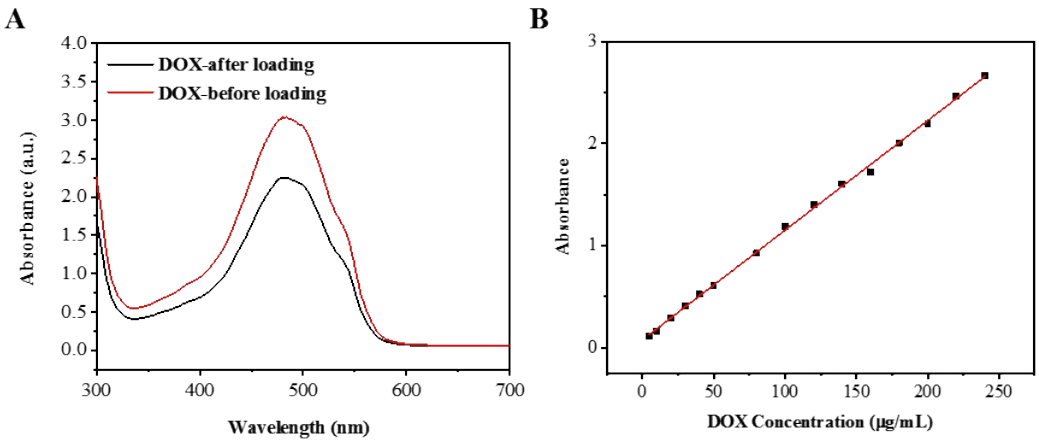

Fig. S12 (A) UV–Vis spectra of DOX solution before and after loading. (B) calibration curve for DOX release study.

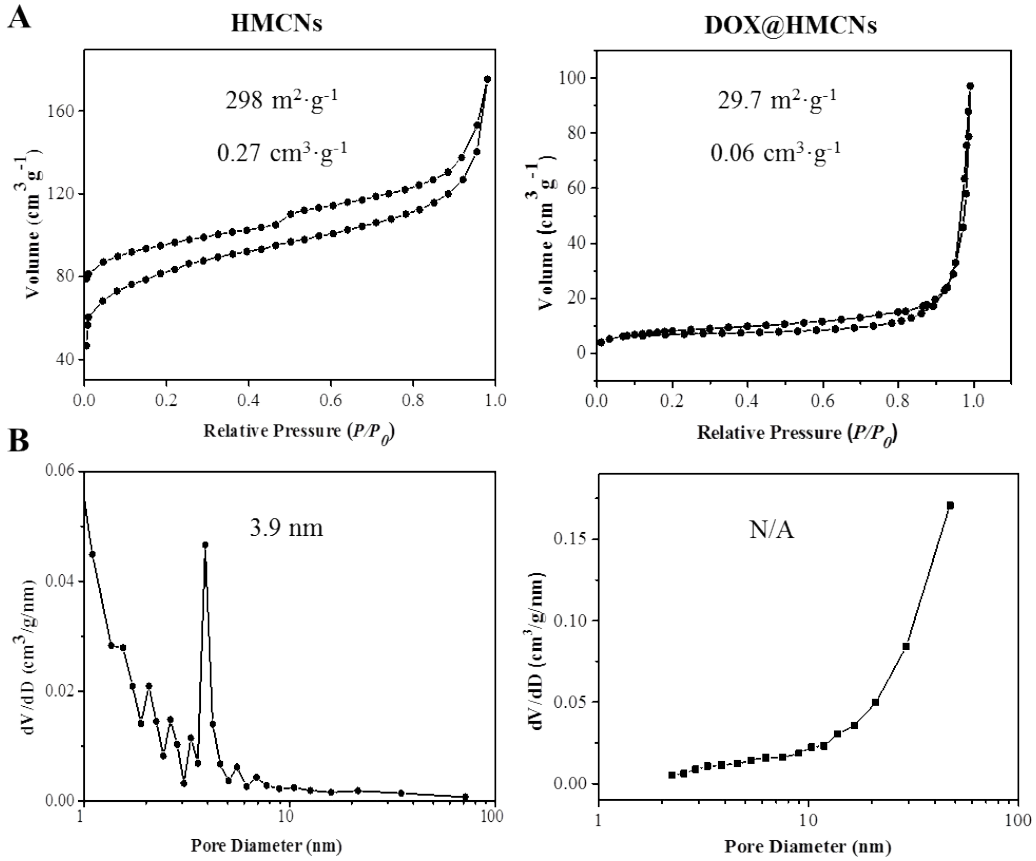

Fig. S13 Nitrogen adsorption/desorption isotherms (A) and pore size distribution (B) of HMCNs and DOX@HMCNs.

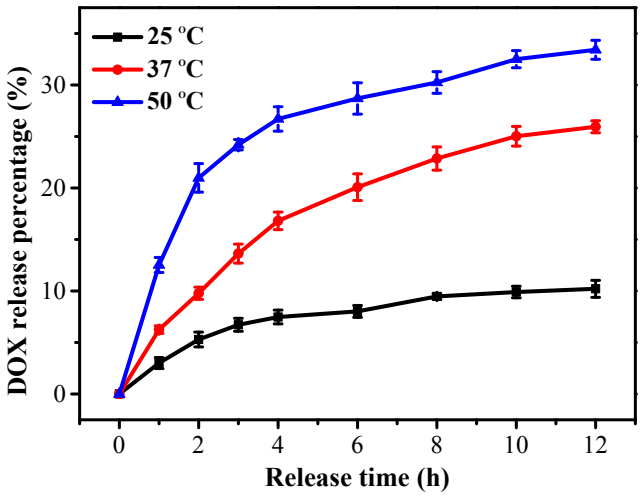

Fig. S14 Cumulative releases of DOX from DOX@HMCNs at pH 6.0 with different temperatures of 25, 37 and 50 ºC.

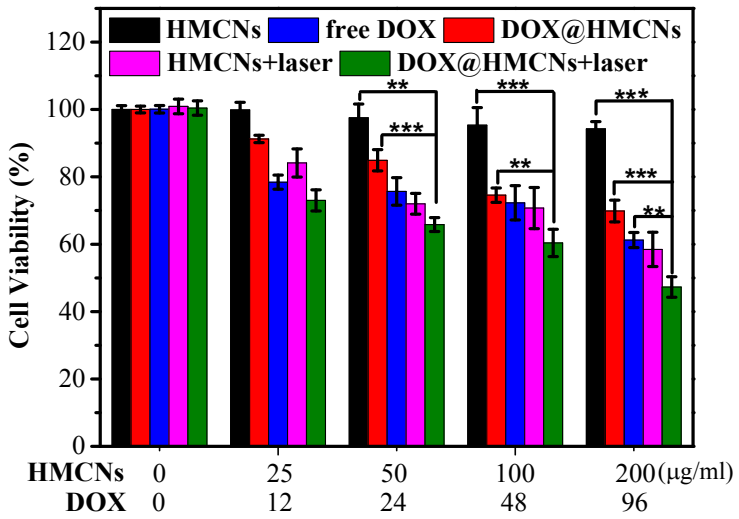

Fig. S15 The concentration-dependent cell viability of U87 MG cells treated with various groups for 4 h (**P<0.01, ***P<0.001).

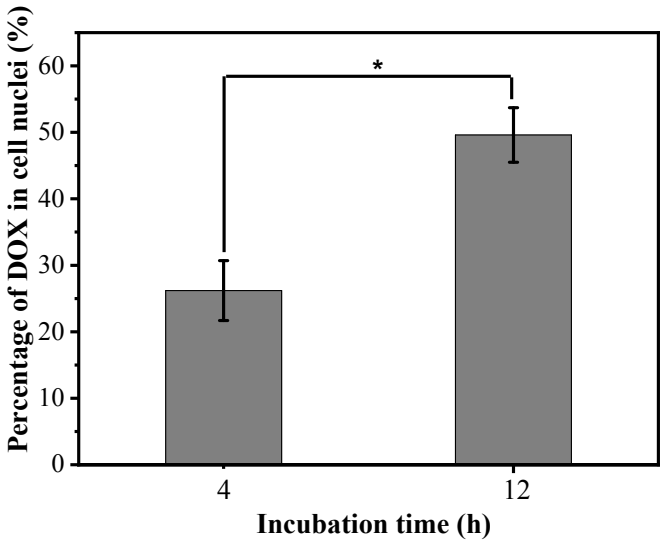

Fig. S16 Percentage of DOX in cell nuclei after 4 and 12 h incubation (*P<0.05).

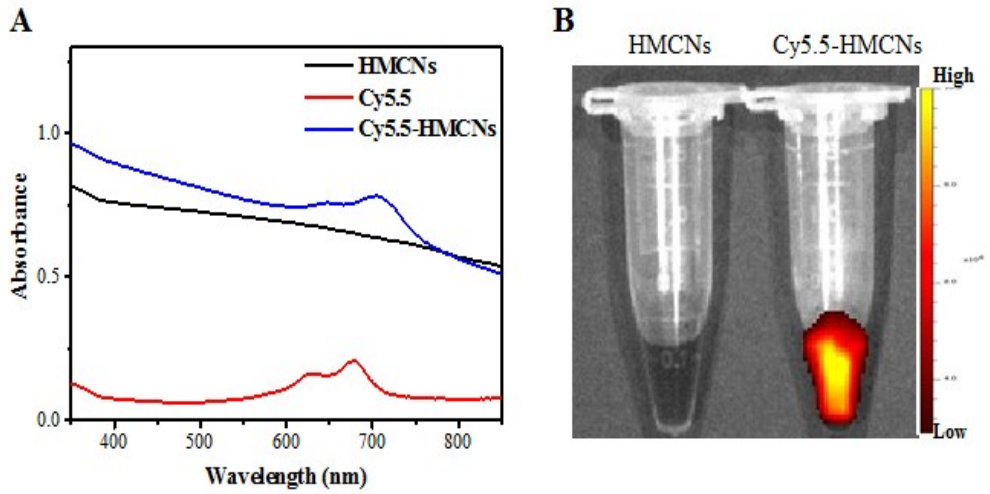

Fig. S17 (A) UV-Vis spectra of Cy5.5, HMCNs and Cy5.5-HMCNs. (B) The fluorescent imaging of HMCNs and Cy5.5-HMCNs.

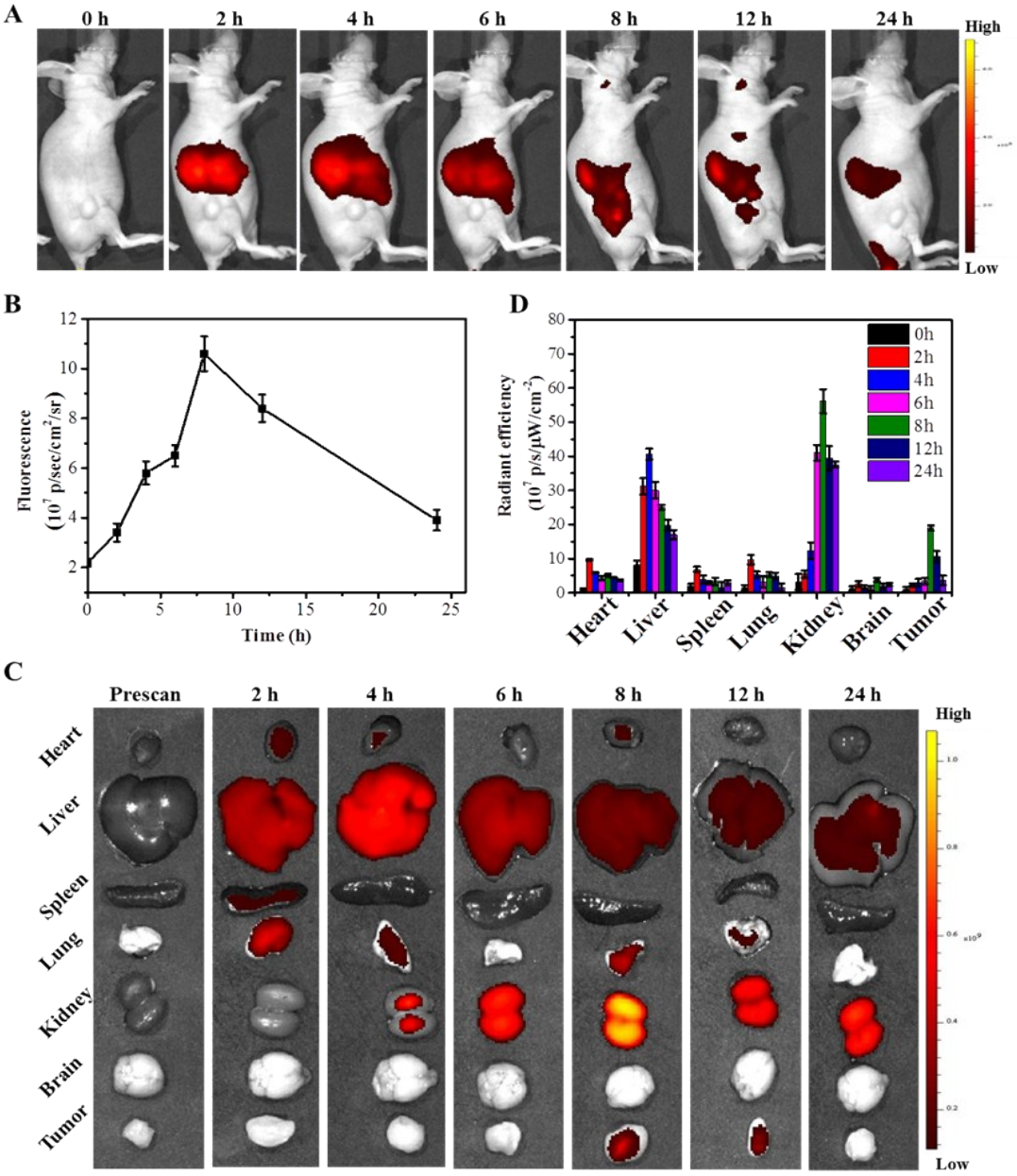

Fig. S18 (A) *In vivo* fluorescence images of U87MG tumor bearing nude mice taken at different time points post i.v. injection of Cy5.5-HMCNs. (B) Fluorescence intensity of tumors at different time points. (C) *Ex vivo* fluorescence images of organs and tumors excised at different time points post i.v. injection of Cy5.5-HMCNs. (D) Quantification of fluorescent signals of each organs and tumors excised at different time points post i.v. injection of Cy5.5-HMCNs.

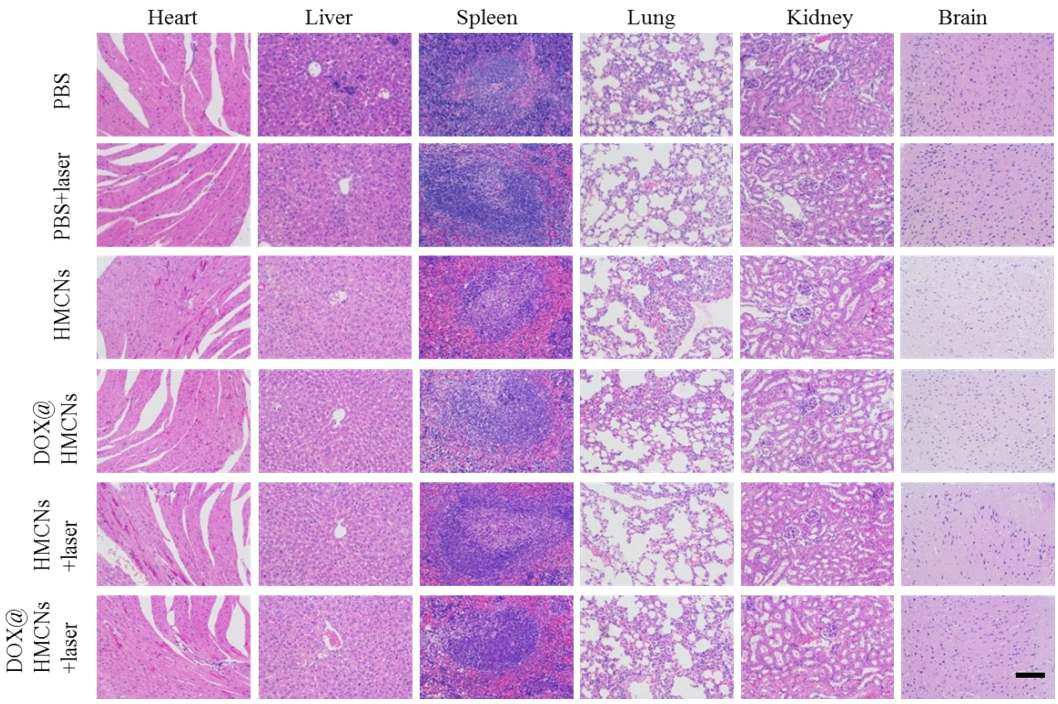

Fig. S19 H&E staining of different tissues collected from mice post various treatments. Scale bar: 100 μm.

References

1. X. J. Liu, B. Li, F. F. Fu, K. B. Xu, R. J. Zou, Q. Wang, B. J. Zhang, Z. G. Chen and J. Q. Hu, *Dalton Trans.*, 2014, **43**, 11709-11715.
2. D. K. Roper, W. Ahn and M. Hoepfner, *J Phys Chem C*, 2007, **111**, 3636-3641.